Flexible-textured polydimethylsiloxane antireflection structure for enhancing omnidirectional photovoltaic performance of $Cu(In,Ga)Se_2$ solar cells

Shou-Yi Kuo,[1,7] Ming-Yang Hsieh,[1] Hau-Vei Han,[2] Fang-I Lai,[3,6,*] Tsung-Yeh Chuang,[4] Peichen Yu,[2] Chien-Chung Lin,[5] and Hao-Chung Kuo[2,8]

[1]*Department of Electronic Engineering, Chang-Gung University,Taoyuan, Taiwan*
[2] *Department of Photonics and Institute of Electro-Optical Engineering, National Chiao-Tung University, Hsinchu, Taiwan*
[3]*Department of Photonics Engineering, Yuan-Ze University, Taoyuan, Taiwan*
[4]*Department of Electro-Physics, National Chiao-Tung University, Hsinchu, Taiwan*
[5]*Institute of Photonic System, College of Photonics, National Chiao-Tung University, Tainan, Taiwan*
[6]*Advanced Optoelectronic Technology Center, National Cheng Kung University, Tainan, Taiwan*
[7]*sykuo@mail.cgu.edu.tw*
[8]*hckuo@faculty.nctu.edu.tw*
**filai@saturn.yzu.edu.tw*

Abstract: Because of the Sun's movement across the sky, broadband and omnidirectional light harvesting is a major development in photovoltaic technology. This study reports the fabrication and characterization of flexible-textured polydimethylsiloxane (PDMS) film on $Cu(In,Ga)Se_2$ (CIGS) solar cells, which is one of the simplest and cheapest peel-off processes for fabricating a three-dimensional structure. A cell containing a textured PDMS film enhanced the short-circuit current density from 22.12 to 23.93 mA/cm^2 in a simulated one-sun scenario. The omnidirectional antireflection of CIGS solar cells containing various PDMS films is also investigated. This study uses an angle-resolved reflectance spectroscope to investigate the omnidirectional and broadband optical properties of the proposed PDMS film. This improvement in light harvesting is attributable to the scattering of the PDMS film and the gradual refractive index profile between the PDMS microstructures and air. The flexible-textured PDMS film is suitable for creating an antireflective coating for a diverse range of photovoltaic devices.

OCIS codes: (040.5350) Photovoltaic; (160.4760) Optical properties.

References and links

1. S. Muthmann and A. Gordijn, "Amorphous silicon solar cells deposited with non-constant silane concentration," Sol. Energy Mater. Sol. Cells **95**(2), 573–578 (2011).
2. M. Kim, S. Sohn, and S. Lee, "Reaction kinetics study of CdTe thin films during CdCl2 heat treatment," Sol. Energy Mater. Sol. Cells **95**(8), 2295–2301 (2011).
3. Chirilă, S. Buecheler, F. Pianezzi, P. Bloesch, C. Gretener, A. R. Uhl, C. Fella, L. Kranz, J. Perrenoud, S. Seyrling, R. Verma, S. Nishiwaki, Y. E. Romanyuk, G. Bilger, and A. N. Tiwari, "Highly efficient $Cu(In,Ga)Se_2$ solar cells grown on flexible polymer films," Nat. Mater. **10**, 1 (2011).
4. L. Zhang, Q. He, W. L. Jiang, F. F. Liu, C. J. Li, and Y. Sun, "Effects of substrate temperature on the structural and electrical properties of $Cu(In,Ga)Se_2$ thin films," Sol. Energy Mater. Sol. Cells **93**(1), 114–118 (2009).
5. EMPA, A new world record for solar cell efficiency, http://www.empa.ch/plugin/template/empa/3/131438/—/l=2, (2013).
6. P. Jackson, D. Hariskos, E. Lotter, S. Paetel, R. Wuerz, R. Menner, W. Wischmann, and M. Powalla, "New world record efficiency for $Cu(In,Ga)Se_2$ thin-film solar cells beyond 20%," Prog. Photovolt. Res. Appl. **19**(7), 894–897 (2011).
7. M. A. Tsai, P. Yu, C. L. Chao, C. H. Chiu, H. C. Kuo, S. H. Lin, J. J. Huang, T. C. Lu, and S. C. Wang,

"Efficiency enhancement and beam shaping of GaN–InGaN vertical-injection light-emitting diodes via high-aspect-ratio nanorod arrays," IEEE Photon. Technol. Lett. **21**(4), 257–259 (2009).
8. Y. A. Chang, Z. Y. Li, H. C. Kuo, T. C. Lu, S. F. Yang, L. W. Lai, L. H. Lai, and S. C. Wang, "Efficiency improvement of single-junction InGaP solar cells fabricated by a novel micro-hole array surface texture process," Semicond. Sci. Technol. **24**(8), 085007 (2009).
9. M. Y. Hsieh, S. Y. Kuo, H. V. Han, J. F. Yang, Y. K. Liao, F. I. Lai, and H. C. Kuo, "Enhanced broadband and omnidirectional performance of Cu(In,Ga)Se2 solar cells with ZnO functional nanotree arrays," Nanoscale **5**(9), 3841–3846 (2013).
10. S. Y. Kuo, M. Y. Hsieh, H. V. Han, F. I. Lai, Y. L. Tsai, J. F. Yang, T. Y. Chuang, and H. C. Kuo, "Dandelion-shaped nanostructures for enhancing omnidirectional photovoltaic performance," Nanoscale **5**(10), 4270–4276 (2013).
11. S. Chhajed, M. F. Schubert, J. K. Kim, and E. F. Schubert, "Nanostructured multilayer graded-index antireflection coating for Si solar cells with broadband and omnidirectional characteristics," Appl. Phys. Lett. **93**(25), 251108 (2008).
12. D. J. Aiken, "High performance anti-reflection coatings for broadband multi-junction solar cells," Sol. Energy Mater. Sol. Cells **64**(4), 393–404 (2000).
13. W. H. Southwell, "Gradient-index antireflection coatings," Opt. Lett. **8**(11), 584–586 (1983).
14. J. A. Dobrowolski, D. Poitras, P. Ma, H. Vakil, and M. Acree, "Toward perfect antireflection coatings: numerical investigation," Appl. Opt. **41**(16), 3075–3083 (2002).
15. D. Poitras and J. A. Dobrowolski, "Toward perfect antireflection coatings. 2. Theory," Appl. Opt. **43**(6), 1286–1295 (2004).
16. J. Zhu, Z. F. Yu, G. F. Burkhard, C. M. Hsu, S. T. Connor, Y. Q. Xu, Q. Wang, M. McGehee, S. H. Fan, and Y. Cui, "Optical absorption enhancement in amorphous silicon nanowire and nanocone arrays," Nano Lett. **9**(1), 279–282 (2009).
17. C. J. Ting, M. C. Huang, H. Y. Tsai, C. P. Chou, and C. C. Fu, "Low cost fabrication of the large-area anti-reflection films from polymer by nanoimprint/hot-embossing technology," Nanotechnology **19**(20), 205301 (2008).
18. B. Päivänranta, T. Saastamoinen, and M. Kuittinen, "A wide-angle antireflection surface for the visible spectrum," Nanotechnology **20**(37), 375301 (2009).
19. Q. Chen, G. Hubbard, P. A. Shields, C. Liu, D. W. E. Allsopp, W. N. Wang, and S. Abbott, "Broadband moth-eye antireflection coatings fabricated by low-cost nanoimprinting," Appl. Phys. Lett. **94**(26), 263118 (2009).
20. E. Oliva, F. Dimroth, and A. W. Bett, "GaAs converters for high power densities of laser illumination," Prog. Photovol. **16**(4), 289–295 (2008).
21. O. Gunawan, K. Wang, B. Fallahazad, Y. Zhang, E. Tutuc, and S. Guha, "High performance wire-array silicon solar cells," Prog. Photovolt. Res. Appl. **19**(3), 307–312 (2011).
22. H. Ng, J. Han, T. Yamada, P. Nguyen, Y. Chen, and M. Meyyappan, "Single crystal nanowire vertical surround-gate field-effect transistor," Nano Lett. **4**(7), 1247–1252 (2004).
23. M. Huang, C. Yang, Y. Chiou, and R. Lee, "Fabrication of nanoporous antireflection surfaces on silicon," Sol. Energy Mater. Sol. Cells **92**(11), 1352–1357 (2008).
24. X.-H. Li, R. Song, Y.-K. Ee, P. Kumnorkaew, J. F. Gilchrist, and N. Tansu, "Light extraction efficiency and radiation patterns of III-nitride light-emitting diodes with colloidal microlens arrays with various aspect ratios," IEEE Photonics Journal **3**(3), 489–499 (2011).
25. X.-H. Li, P. Zhu, G. Liu, J. Zhang, R. Song, Y.-K. Ee, P. Kumnorkaew, J. F. Gilchrist, and N. Tansu, "Light extraction efficiency enhancement of III-nitride light-emitting diodes by using 2-D close-packed TiO microsphere arrays," J. Display Technology **9**(5), 324–332 (2013).
26. W. H. Koo, W. Youn, P. Zhu, X.-H. Li, N. Tansu, and F. So, "Light extraction of organic light emitting diodes by defective hexagonal-close-packed array," Adv. Funct. Mater. **22**(16), 3454–3459 (2012).
27. Y.-K. Ee, P. Kumnorkaew, R. A. Arif, H. Tong, J. F. Gilchrist, and N. Tansu, "Light extraction efficiency enhancement of InGaN quantum wells light-emitting diodes with polydimethylsiloxane concave microstructures," Opt. Express **17**(16), 13747–13757 (2009).
28. K. Sato, M. Shikida, T. Yamashiro, K. Asaumi, Y. Iriye, and M. Yamamoto, "Anisotropic etching rates of single-crystal silicon for TMAH water solution as a function of crystallographic orientation," Sens. Actuators **73**(1-2), 131–137 (1999).
29. J. Zhong, H. Chen, G. Saraf, Y. Lu, C. K. Choi, J. J. Song, D. M. Mackie, and H. Shen, "Integrated ZnO nanotips on GaN light emitting diodes for enhanced emission efficiency," Appl. Phys. Lett. **90**(20), 203515 (2007).

1. Introduction

Solar energy is the most renewable and secure energy among existing energy sources. Because of the global warming effect and energy crisis, solar energy has become a major topic of research in recent years. Solar cells can be roughly divided into bulk- and thin-film devices, based on their structures. The thin-film materials include CdTe, amorphous silicon, and Cu(In,Ga)Se_2 (CIGS) [1,2]. Among all thin-film solar cells, CIGS and related materials

#200954 - $15.00 USD Received 7 Nov 2013; revised 10 Jan 2014; accepted 10 Jan 2014; published 31 Jan 2014

possess great potential because of a high optical absorption, adjustable band-gap, and stable photo-degradation [3,4]. Recent research has revealed that the conversion efficiencies of the CIGS solar cells at the laboratory scale have exceeded 20% [5,6].

Antireflective coatings (ARCs) are applied to the surface of a material to reduce Fresnel reflection loss at the interface between the materials, which plays a crucial role in solar cells [7–11]. Conventional multilayer ARCs and biomimetic moth-eye structures have mainly been used [12–19]. However, the multilayer ARCs possess some disadvantages, such as material selection, layer thickness control, thermal expansion mismatch, and material diffusion [20]. The biomimetic moth-eye structures exhibit excellent broadband and omnidirectional antireflection characteristics, but the fabrication processes are not suitable for mass production of nanostructures on large-area solar cells and the process-induced surface-recombination defects degrade the device performance [21–23].

Prior works have also reported on the use of self-assembled colloidal microlens arrays in 2-D close-packed configurations for reducing the reflectance at the semiconductor / air interface [24, 25], In addition, the use of this colloidal template had also been implemented as the imprinting mold for forming concave microstructures in PDMS template for reducing the reflection and increasing escape cone in semiconductor / air interface [26, 27]. This study demonstrates a platform to combine the flexible-textured polydimethylsiloxane (PDMS) film with CIGS solar cells. The PDMS film provides a refractive index gradient to reduce Fresnel reflection loss as an antireflection layer. The advantages of using a PDMS film as an antireflection layer are the low-cost nonvacuum system and simple process. This study experimentally investigated the optical properties of two types of PDMS films: flat and textured. By fabricating the different structures, the varied profiles of effective refractive index could be obtained. The results of CIGS solar cells to which both types of antireflection layers had been applied were compared with cells possessing only a bare layer. The power conversion efficiency of the CIGS solar cell possessing the PDMS film can be effectively improved compared to a bare solar cell because of the enhanced antireflective (AR) properties.

2. Experimental

The multilayered structure of the CIGS solar cell was fabricated using Mo/CIGS/CdS/i-ZnO/Al-doped ZnO (AZO) on a soda-lime glass substrate, as shown in Fig. 1(a). First, the approximately 1-μm-thick Mo electrode was deposited using the direct current magnetron sputtering system. The approximately 2-μm-thick CIGS absorber layer was deposited by employing the co-evaporation technique. The buffer layer of the 50–60 nm-thick CdS was then deposited using the chemical bath deposition technique. A highly resistive i-ZnO layer between the CdS and ZnO:Al layers was deposited using radio frequency (RF) magnetron sputtering to reduce the leakage current. Finally, the 600 nm-thick AZO layer was deposited by RF magnetron sputtering and the top electrode of the Al grid was deposited by thermal evaporation as a transparent conducting oxide.

To prepare a flexible-textured PDMS film, first, the randomly crystalline silicon (c-Si) mold was fabricated by wet-etching in potassium hydroxide. The detailed fabrication of wet-etching process of c-Si mold was reported in the previous paper [28]. To manufacture the PDMS film, the base to cross-linking agent mass ratio was 10:1. The PDMS pre-polymer solution was poured onto the textured mold-pattern surface. To form a uniform PDMS layer, the c-Si mold-pattern was filled using a spin coating method. A 50 micron layer of PDMS was the spin-coated on c-Si mold at 500 rpm for 60 seconds. The PDMS-coated c-Si mold was heated to a temperature of 100°C for one hour. After being detached from the c-Si mold, a flexible-textured PDMS film was successfully obtained.

#200954 - $15.00 USD Received 7 Nov 2013; revised 10 Jan 2014; accepted 10 Jan 2014; published 31 Jan 2014

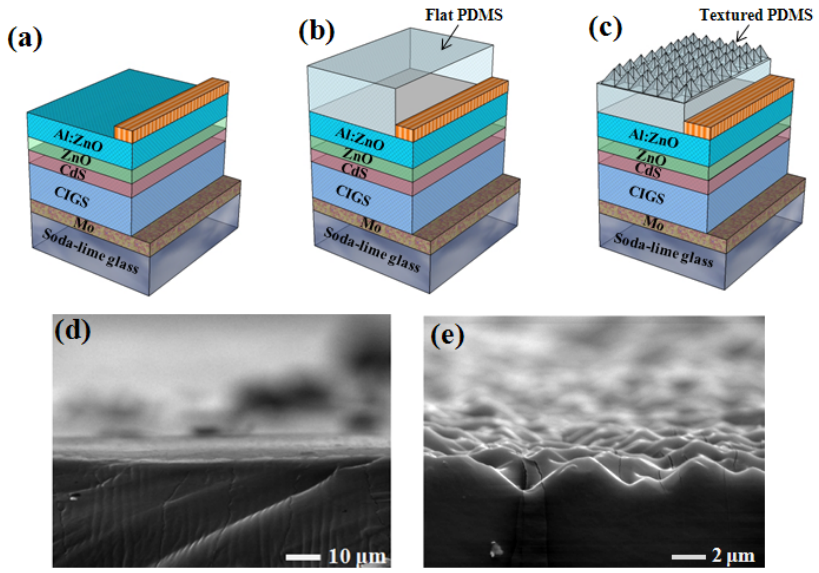

Fig. 1. A schematic plot of the fabricated CIGS solar cell with flat and flexible textured PDMS. (a)Bare cell. (b) Cell with flat PDMS film. (c) Cell with textured PDMS film. (d) SEM image of flat PDMS film. (e) SEM image of randomly textured PDMS film.

Finally, the flexible PDMS film was layered onto the surface of the CIGS solar cell, as shown in Figs. 1(b) and 1(c). Figures 1(d) and 1(e) show the scanning electron microscopy (SEM) images of the flat and textured PDMS films, in which the height of the textured random structure was approximately 2.5 μm.

The morphologies of the flexible PDMS films on soda-lime glass substrates were observed using field emission scanning electron microscopy (FESEM, Hitachi S-4700I). To characterize the omnidirectional optical performance of the PDMS film, it was layered on CIGS solar cells and the angle-dependent reflectance of the cells was measured with a 15cm-radius integrating sphere to collect the scattered photons, a broadband 300W Xenon lamp and analyzed by a spectrometer. The sample stage was placed in the center of the integrating sphere titled at 8 degree with x-y plane. For angular dependent reflectance, the sample stage was kept at 8 degree with x-y plane, and rotated from −60 to 60 degree about the z-axis. The power conversion efficiencies of CIGS solar cells were measured under a simulated AM1.5G illumination exhibiting a power of 1,000 W/m^2. The results of external quantum efficiency (EQE) were acquired using a 300 W Xenon lamp (Newport 66984) light source and a monochromator (Newport 74112). The spectrum of the EQE was measured at wavelengths ranging from 400 to 1,000 nm. The temperature was maintained at 25 ± 1 °C during the measurements.

3. Result and disscusion

To determine the AR performance of the flat and textured PDMS structures in the 400–1,000 nm range, the reflectance spectrum was measured for normal light incidence with a standard UV-vis spectrometer and an integrating sphere, as shown in Fig. 2(a). The result indicates that the flat PDMS and textured PDMS attached to the surfaces of CIGS solar cells, causing the principle reflectance to decrease. The mean reflectance of the bare CIGS cells was approximately 6.78%, whereas the mean reflectance of the CIGS cell with a flat PDMS film on the surface had decreased to 4.63%. Finally, the mean reflectance decreased to 2.30% when the textured PDMS film was layered on the surface. Attaching the textured PDMS film to the CIGS cell surface caused the reflectance to decrease at every wavelength. Therefore,

#200954 - $15.00 USD Received 7 Nov 2013; revised 10 Jan 2014; accepted 10 Jan 2014; published 31 Jan 2014

this study proposes that the textured PDMS is suitable for wavelength-independent AR coatings for CIGS solar cells.

Figure 2(b) displays the textured PDMS film pasted on the surface of bare CIGS solar cells, as shown in the upper-right corner of the cell. The reflection characteristics were investigated by examining the reflection of the words printed on the paper imaged on the cell. The textured PDMS film degraded the brightness of the reflection characteristics compared to the bare cell. Moreover, the color of the cell possessing a textured PDMS film was much blacker than that of the bare cell. This result is in agreement with the reflectance shown in Fig. 2(a).

Because of the Sun's movement, the antireflection coating should increase the transmission into the absorption layer and reduce reflection omnidirectionally. To understand the omnidirectional AR characteristics, this study measured the angle-dependent reflection of

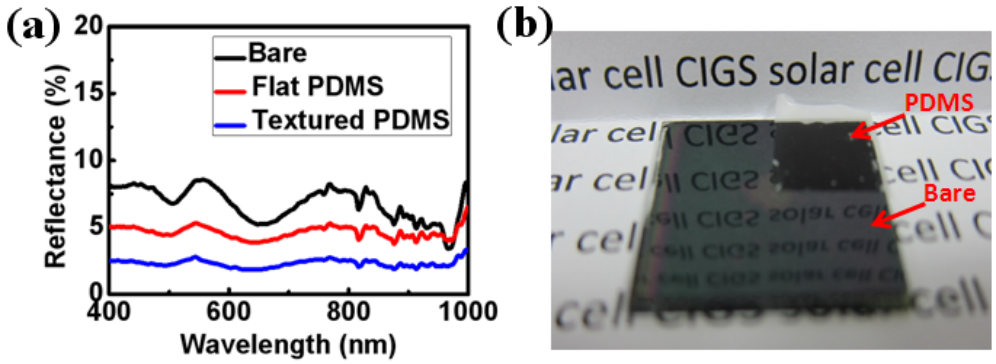

Fig. 2. (a) Reflectance measurements of the flat PDMS and textured PDMS on CIGS solar cells compare with bare one. (b) Images of (right) CIGS solar cell with textured PDMS film and (left) bare CIGS solar cell

the CIGS solar cells with the PDMS films. Figures 3(a)–3(c) show the measured angle-dependent reflectance of CIGS solar cells possessing flat PDMS films, the textured PDMS films, and the bare cell. The angle-dependent mappings of the CIGS solar cells were performed at wavelengths from 400 to 1,000 nm and at incident angles ranging from −60° to 60°. Figure 3(a) shows that the bare cell exhibited higher reflection at 55°–60° and the amplitude of the interference fringe was in the visible range. When a flat-PDMS film was pasted on the CIGS cell surface, the reflection decreased omnidirectionally. The different reflectance behaviors are attributable to the scattering of the PDMS film and the gradual refractive index profile between the PDMS microstructures and the air. To further investigate the effect of the solar power harvest, the solar-spectrum (AM1.5G) weighted reflectance (SWR) was estimated by the solar spectral photon flux and the reflectance spectra integrated in a wavelength range from 400 nm to 1,000 nm. Here, we define the SWR as the following:

$$\mathrm{SWR} = \frac{\int_{400\,\mathrm{nm}}^{1000\,\mathrm{nm}} R(\lambda) I_{\mathrm{AM1.5G}}(\lambda)\,d\lambda}{\int_{400\,\mathrm{nm}}^{1000\,\mathrm{nm}} I_{\mathrm{AM1.5G}}(\lambda)\,d\lambda} \quad (1)$$

where $R(\lambda)$ is the measured reflectivity and $I_{AM1.5G}$ is the photon flux density of the AM1.5G solar spectrum. The weight reflectance of the bare CIGS cell was approximately 6.97%, whereas the weight reflectance of the CIGS cell with the flat PDMS film attached to the surface decreased to 4.63%. Finally, the weight reflectance decreased to 2.29% when the textured PDMS film was layered on the surface of the CIGS solar cell. Figure 3(d) shows the weighted reflectance of the textured PDMS cell, exhibiting a dramatic decrease at every incident angle compared to the bare cell and flat PDMS cell. The weighted reflectance of the

#200954 - $15.00 USD Received 7 Nov 2013; revised 10 Jan 2014; accepted 10 Jan 2014; published 31 Jan 2014

textured PDMS cell is still less than 4% at an incident angle of 45°, and 5% at an incident angle of 60°.

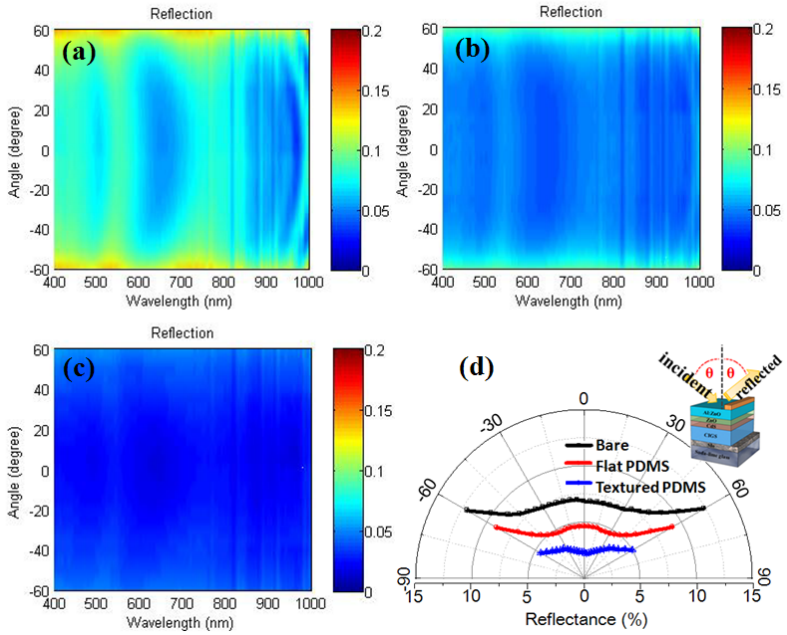

Fig. 3. The measured angular reflectance spectra for solar cell with (a)Bare (b)flat PDMS film (C) textured PDMS film.(d)The weighted reflectance of all cells, calculated by the measured angular reflectance spectra shown in (a)-(c). The inset in (d) is a schematic of the angle dependence between incident and reflected lights.

The PDMS is optically clear, especially in the solar spectra regime. Though the interference effect due to thickness variation can't be completely ruled out, it is reasonable to exclude the absorption from the reduction in reflectance. In this paper, we kept the same thickness of PDMS films, and concentrated the discussion on the enhanced antireflective properties due to textured surface. The different reflectance behaviors are attributable to two possible explanations. First, because of the scattering of the PDMS film, the light path length can be increased when compared with the CIGS solar cell without a PDMS film. Second, the reflectance behaviors are caused by the gradual refractive index profile between the PDMS microstructures and the air. In previous theoretical studies, the AR structure was comprised of multilayer stacks and the effective medium theory (EMT) was adopted to describe the optical properties [29]. In this study, the refractive index decreased gradually from the AR material to the air. Therefore, the EMT adopted to explain the reflection can be efficiently reduced by the textured PDMS film. The AR structure prevents reflected wavelengths by using different optical interfaces to cancel each wavelength partially or wholly through destructive interference. Particularly because of the enhanced destructive interferences, the reflectance may decrease in cells possessing a textured PDMS film. In addition, based on previous research, the reflectance of a single-layer AR coating is higher than the gradient-index AR coating and the bandwidth of the gradient-index AR coating may broaden. This phenomenon originates from the fact that the gradient-index AR coating is suitable for AR coating because of the smoother grading in the refractive index. In this study, the flat PDMS film can be treated as an effective single layer, and the PDMS microstructures on the textured film play the role of a graded layer, alleviating the drastic change in the refractive index between the air and PDMS film. The effective refractive index (n_{eff}) of the PDMS microstructures can be obtained with the weighting formula as follows:

#200954 - $15.00 USD Received 7 Nov 2013; revised 10 Jan 2014; accepted 10 Jan 2014; published 31 Jan 2014

$$n_{eff} = [n_{PDMS}^2 \times f + n_{air}^2 (1-f)]^{\frac{1}{2}} \quad (2)$$

where f is the filling factor of PDMS microstructures, and n_{PDMS} and n_{air} are refractive indexes of PDMS and air, respectively. In these calculations, the refractive index of PDMS is approximately 1.4 and the filling factor is estimated from the SEM images, as shown in Fig. 1(e). For the unit PDMS microstructures, the filling factors of the top and bottom of the PDMS structures were 0 and 1, respectively, and the n_{eff} values were calculated as 1 and 1.4, respectively. Because of the variation in length of the PDMS microstructures, the microstructure filling factor varies with the depth. The calculated refractive index profiles are plotted in Fig. 4. As shown in Fig. 4, the flat PDMS film exhibited equivalent two-step refractive index profiles, and the textured PDMS film exhibited equivalent three-step refractive index profiles, thus adding a gradual step where the refractive index of PDMS microstructures exhibited nearly exponentially increased from planar PDMS to the air. Therefore, cells with textured PDMS films exhibit the lowest reflection because of the scattering of the PDMS film and a smoother grading in the effective refractive index profile from the air to the surface of the cell (the refractive index of AZO is approximately 2.1) than in both the bare CIGS cells and in cells possessing a flat PDMS film.

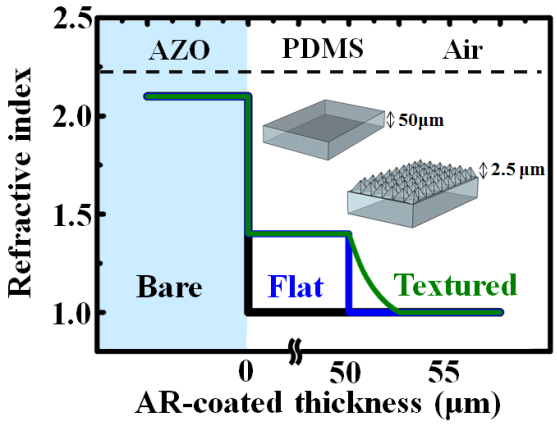

Fig. 4. Schematic illustration of the refractive index profiles of different PDMS films AR-coated on CIGS solar cells with varying AR-coated thickness.

Figure 5 shows the IV curve and the external quantum efficiency (EQE) of solar cells processed with and without a textured PDMS film. The bare CIGS solar cells and the cells possessing textured PDMS films exhibited conversion efficiencies (η) of 9.4% and 10.21% with approximate open-circuit voltages (V_{oc}) of 0.64 V and a fill factor (FF) of 0.66, and Jsc of 22.12mA/cm^2 and 23.93 mA/cm^2, respectively. Thus, the photovoltaic efficiency is enhanced because J_{sc} of the CIGS solar cell possessing a textured PDMS film was greater than that of the bare cell. The photocurrent enhancement factor (EF_{jsc}) was 8.18%, as calculated by the following equation:

$$EF_{jsc} = \frac{\Delta Jsc}{Jsc} = \frac{Jsc(\text{with ARc}) - Jsc(\text{without ARc})}{Jsc(\text{without ARc})} \quad (3)$$

The enhancement of the conversion efficiency of the cells possessing textured PDMS films is also supported by the EQE measurement, as shown in Fig. 5(b). Compared with the bare cell, the EQE of the CIGS solar cell possessing a textured PDMS film revealed an enhanced photoresponse for wavelengths ranging from 400 to 1,000 nm, which is consistent with the reduced reflectance at the same wavelength range. This observation confirms that the enhancement in Jsc of the CIGS solar cell possessing textured PDMS films compared with

#200954 - $15.00 USD Received 7 Nov 2013; revised 10 Jan 2014; accepted 10 Jan 2014; published 31 Jan 2014

that of the bare cell is because of the broadband antireflection property of the textured PDMS film. Consequently, the flexible-textured PDMS film is expected to be a suitable alternative AR layer for diversity photovoltaic devices in the future.

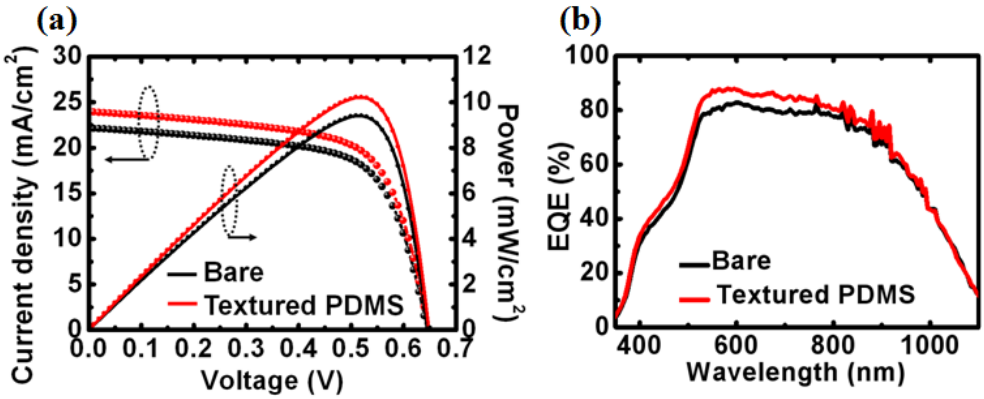

Fig. 5. (a) The current density-voltage curves and (b) the external quantum efficiencies of the solar cell with textured PDMS film and the bare cell.

4. Conclusion

In conclusion, a CIGS solar cell possessing a textured PDMS film was fabricated and characterized in detail. The study demonstrated that the textured PDMS film possesses superior AR properties across a broad spectral range and angles of incidence. Because the structures can reduce surface Fresnel reflection, the weight reflectance of the bare CIGS solar cells and the cells possessing the textured PDMS film were 6.97% and 2.29%, respectively. Moreover, the photocurrent density increased from 22.12 to 23.93 mA/cm^2, differing by an additional 1.81 mA/cm^2. The conversion efficiency increased from 9.4% to 10.21%. Because of the low-temperature and cost-efficient fabrication process, this study proposes the textured PDMS film as a suitable alternative AR layer for other electro-optical devices.

Acknowledgments

This work was also supported by the Green Technology Research Center of Chang Gung University and the National Science Council (NSC) of Taiwan under contract no.s NSC101-2112-M-182-003-MY3 and NSC101-3113-E-182-001-CC2.